

Supplementary Information for Cholesterol enhances influenza binding avidity by controlling nanoscale receptor clustering

Supplementary Methods:

Chemicals. Dioleoyl phosphatidylethanolamine (DOPE), Palmitoyl oleoyl phosphatidylcholine (POPC), cholesterol, stigmasterol, 7-dehydrocholesterol, desmosterol, and lanosterol were all purchased from Avanti Polar Lipids (Alabaster, AL). 5-cholesten-3-one and ergosterol were purchased from Sigma-Aldrich (St. Louis, MO). The viral target receptor, disialoganglioside GD1a from bovine brain (Cer-Glc-Gal(NeuAc)-GalNAc-Gal-NeuAc), was also purchased from Sigma-Aldrich. Fluorophores Texas Red-1,2-dihexadecanoyl- *sn*-glycero-3-phosphoethanolamine (TR-DHPE) and Oregon Green-1,2-dihexadecanoyl- *sn*-glycero-3-phosphoethanolamine (OG-DHPE) were purchased from Thermo Fisher Scientific (Waltham, MA).

Dissociation Rate Analysis in Simulations. As described previously¹, dissociation was modeled as a two-state reaction which follows a Poisson distribution and thus has the following probabilities:

$$P_{dissociate}(t = \tau | k_{off}) = k_{off} e^{-k_{off} \tau}$$

$$P_{stay}(t = 0, \dots, \tau | k_{off}) = e^{-k_{off} \tau}$$

Contact lifetime analysis result in a set of N identified contact events, n of which terminate by the end of the simulation with lengths $[t_1, \dots, t_n]$ and $N-n$ of which are still in contact at the end of the simulation with partial contact lifetimes with lengths $[T_1, \dots, T_{N-n}]$. Assuming a uniform prior for k_{off} , the probability density function for k_{off} thus follows:

$$P(k_{off} | N, t_1, \dots, t_n, n, T_1, \dots, T_{N-n}) = \frac{\theta^{n+1}}{n!} k_{off}^n \exp(-k_{off} \theta)$$

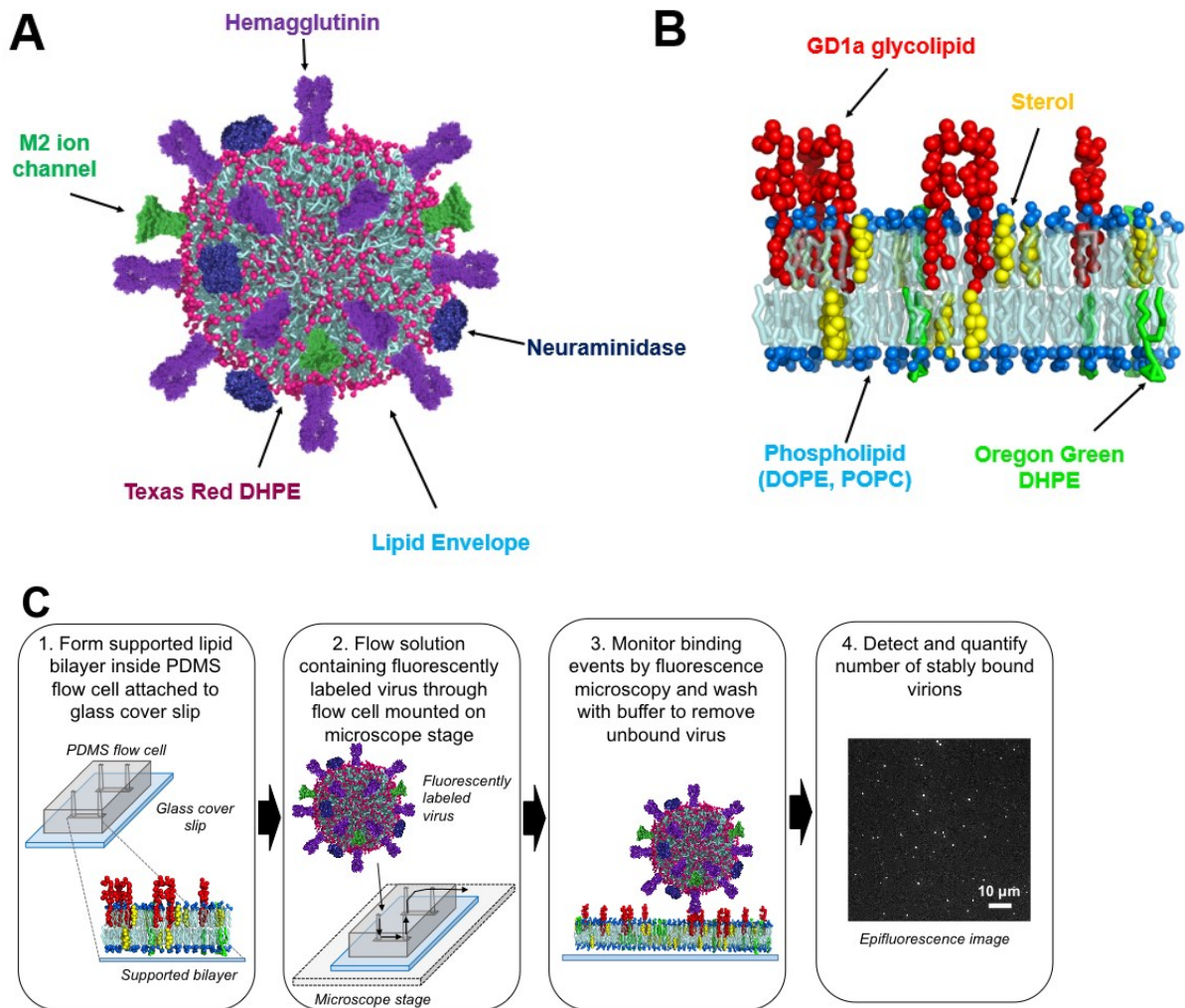
$$\theta = \sum_{i=1}^n t_i + \sum_{j=1}^{N-n} T_j$$

where

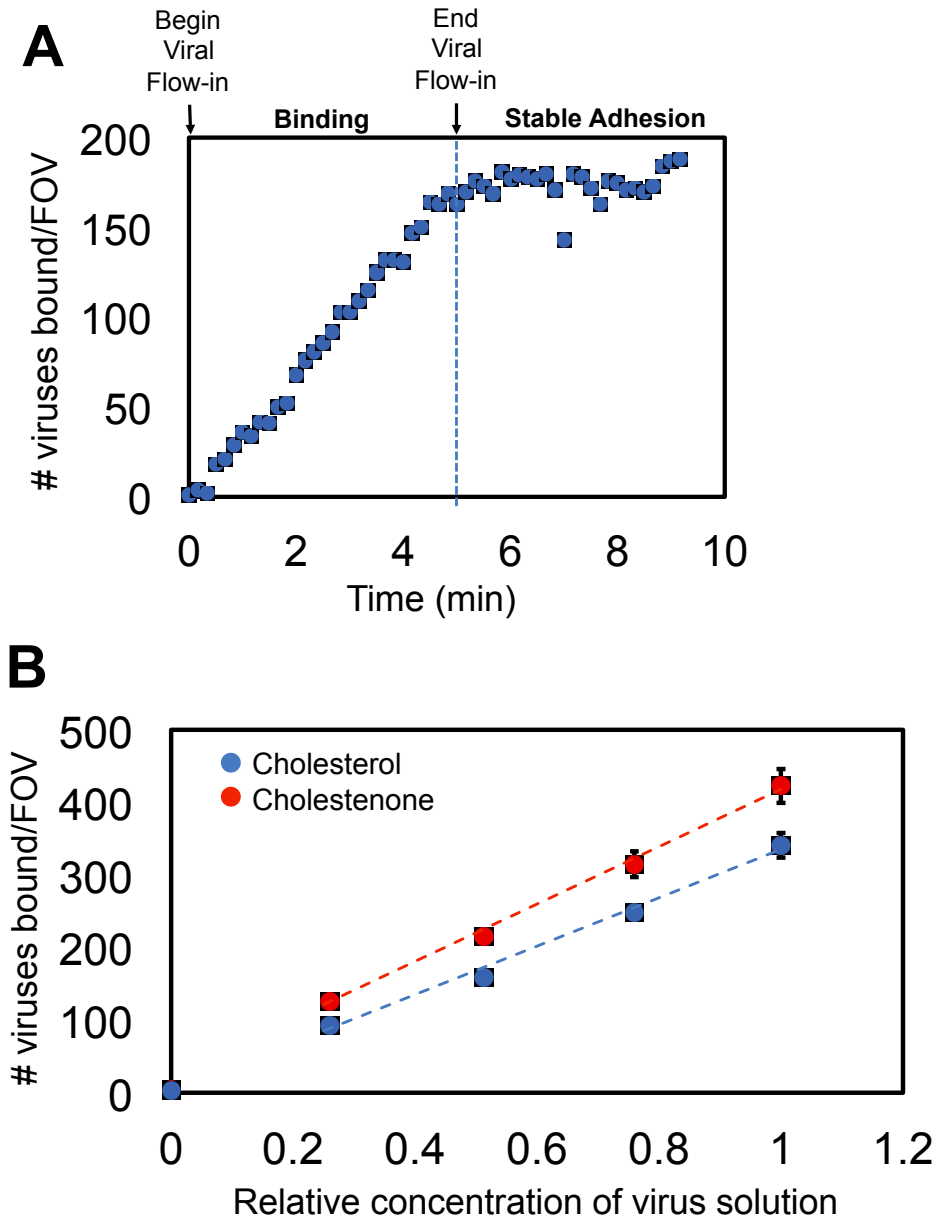
Mol % Cholesterol	Mol % GD1A				Membrane Component
	1 mol %	2 mol %	4 mol %	10 mol %	
0 mol %	3	7	14	36	GD1a
	72	72	72	72	DOPE
	285	281	274	252	POPC
	19049	18794	18383	17146	PW
10 mol %	3	7	14	36	GD1a
	36	36	36	36	CHOL
	72	72	72	72	DOPE
	249	245	238	216	POPC
	19199	18929	18563	17270	PW
20 mol %	3	7	14	36	GD1a
	72	72	72	72	CHOL
	72	72	72	72	DOPE
	212	209	202	180	POPC
	19351	19061	18634	17338	PW

Supplementary Table 1: Table of simulated lipid bilayer compositions.

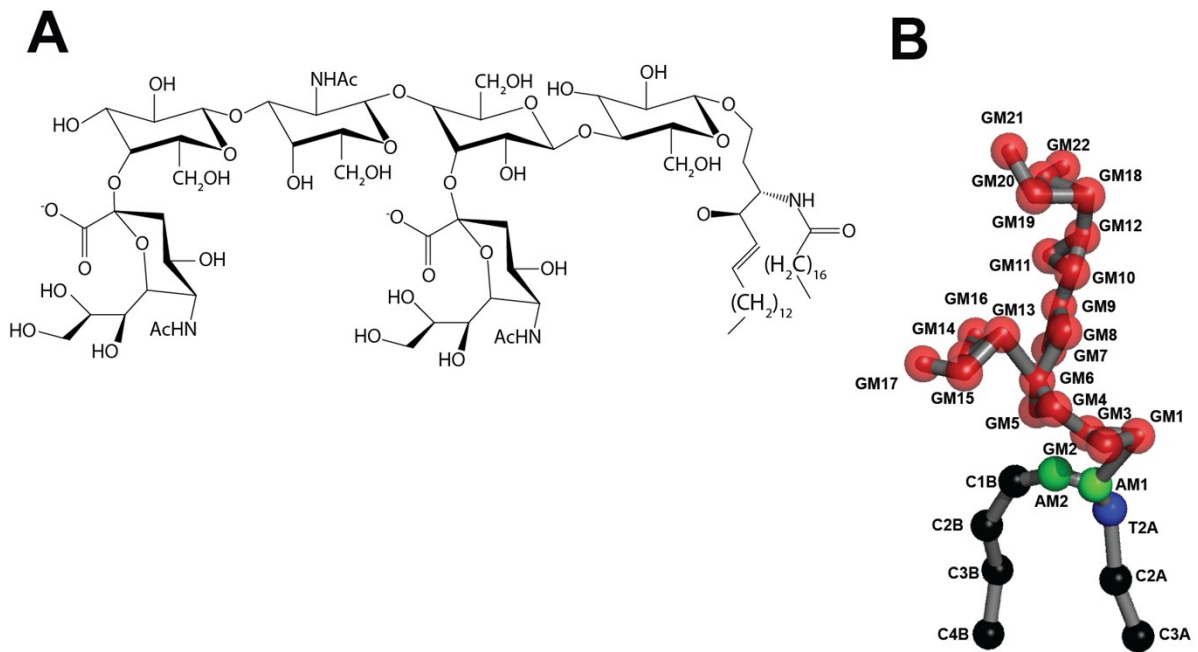
Listed values represent the number of phospholipids (DOPE, POPC), GD1a and cholesterol (CHOL) molecules present in each monolayer of each bilayer simulation. In all experimental conditions, the mol % of DOPE was held constant at 20 mol %. GD1a concentration was varied between 1, 2, 4 and 10 mol % and cholesterol was varied between 0, 10 and 20 mol %. The remaining mol % was POPC. Membranes of each composition were constructed with INSANE², and then the simulation box was solvated with a polarizable water model (PW) and 150 mM NaCl.



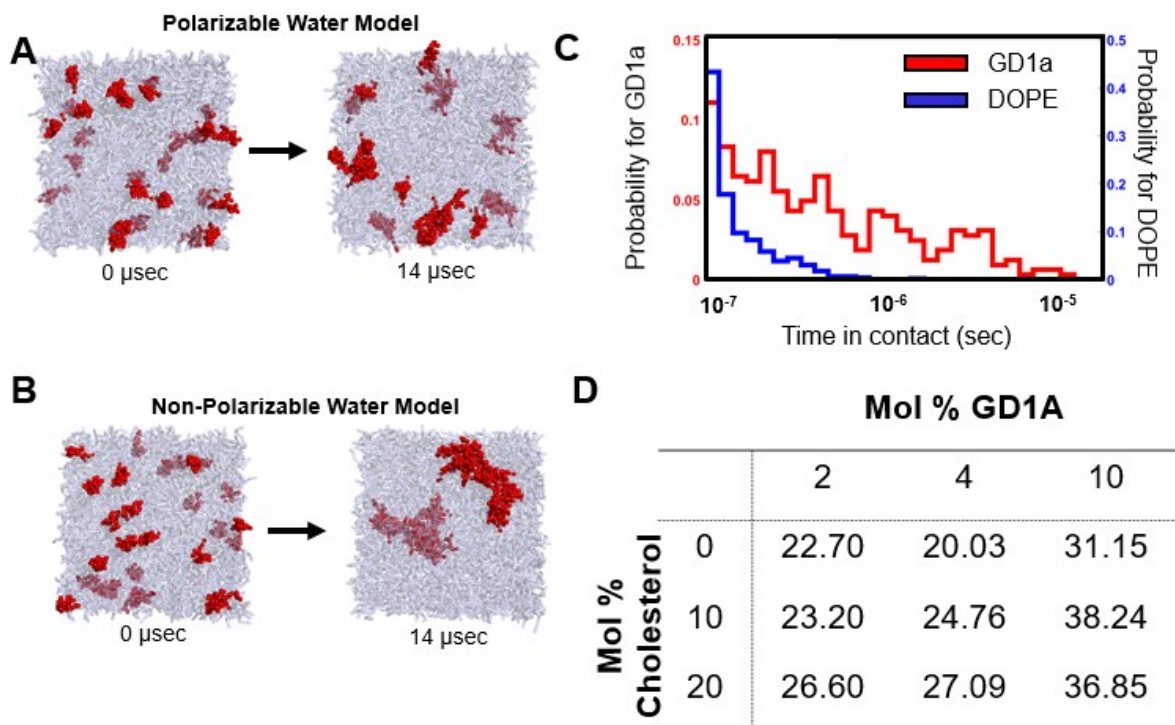
Supplementary Figure 1: Schematics of virus, bilayer, and in-vitro binding assay. An influenza virion is schematized in part (A), a target bilayer in part (B), and the single-virion binding assay in part (C). We do not detect a preferential association of cholesterol with GD1a versus phospholipids in simulations of supported lipid bilayers with compositions matching those used experimentally.



Supplementary Figure 2: Viral binding to target membranes is linear as a function of time and viral concentration. Viral binding is plotted as a function of time (A) as measured via fluorescence microscopy. A virus-containing solution was flowed through an imaging chamber containing a target membrane with 10 mol % cholesterol at a constant rate for 5 minutes (dotted line). At 5 minutes, the imaging chamber was washed with virus-free buffer. Binding increased in a linear fashion over time and did not reach saturation within the experimental time window. Once bound, virions remained stably attached to the target membrane. Viral binding is also plotted as a function of viral concentration after 2.5 minutes of incubation (B) with target membranes containing 10 mol % cholesterol (blue) or cholestenone (red). Results are representative of conditions tested using the single-virus binding assay.

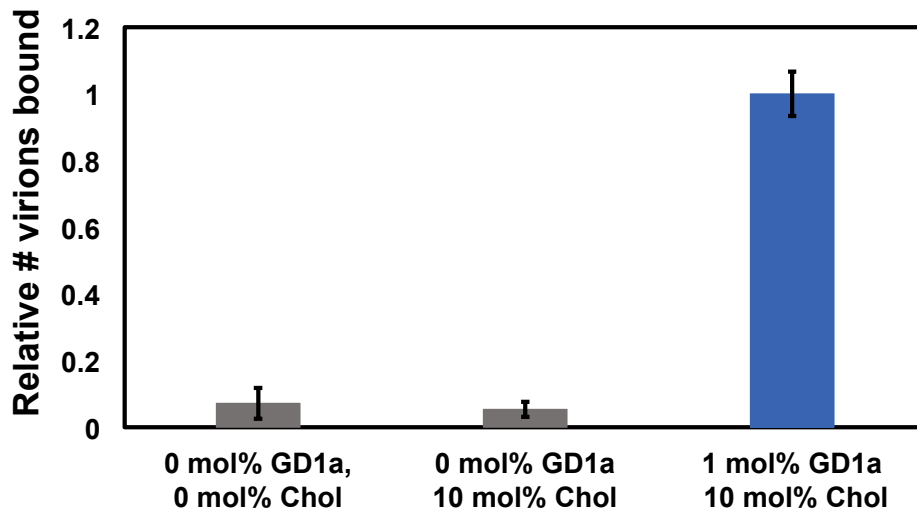


Supplementary Figure 3: Chemical structure of GD1a (A) and GD1a topology constructed with MARTINI beads for coarse-grained MD simulations (B).

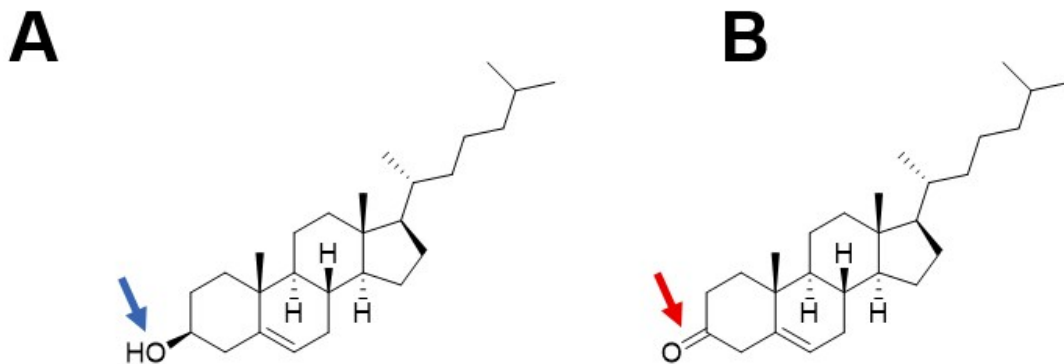


Supplementary Figure 4: Dynamic association-dissociation behavior of simulated GD1a molecules in membranes.

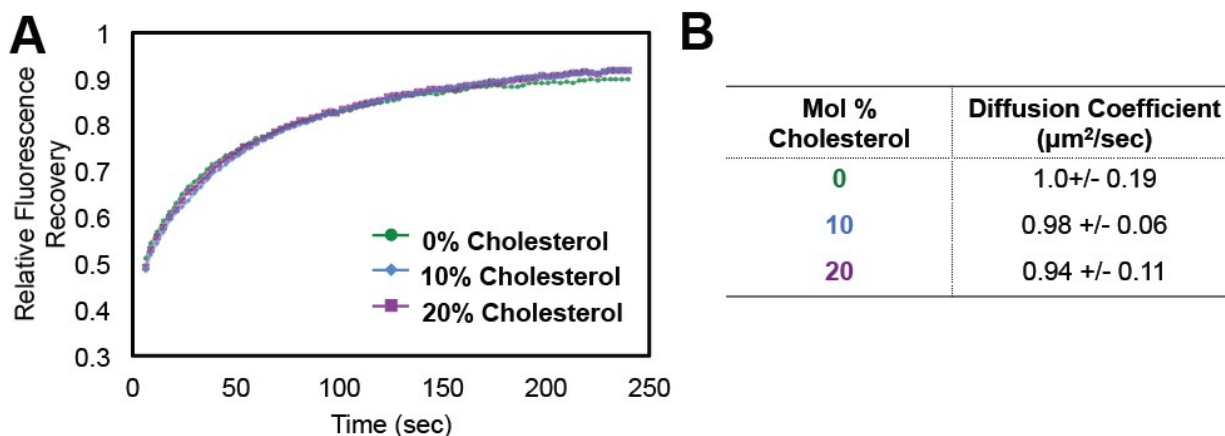
(A) Snapshots of membrane containing 4 mol% GD1a and no sterol simulated with a polarizable water model. The use of a polarizable CG water model drastically reduced artificial, simulation-induced clustering. Snapshots are representative of 4 mol% GD1a simulations with 0, 10 or 20 mol% cholesterol. Red = GD1a; Grey=Phospholipids. (B) Snapshots of membranes containing 4 mol% GD1a and no sterol simulated with a non-polarizable water model. A single cluster of all GD1a formed and remained throughout the simulation. (C) Histogram of contact lifetimes between GD1a pairs (blue) and DOPE pairs (red) for simulated membranes containing 4 mol% GD1a and 10 mol% cholesterol. GD1a shows preferential self-association, and pairwise GD1a-GD1a contacts persist significantly longer than phospholipid-phospholipid contacts do. (D) Table of mean contact lifetimes in nanoseconds between GD1a pairs at different mol% GD1a and cholesterol. For membranes containing 2, 4 or 10 mol% GD1a, cholesterol increases mean lifetime.



Supplementary Figure 5: Negligible viral binding occurs in the absence of GD1a receptor. Relative viral binding to target membranes containing no GD1a and either 0 mol% or 10 mol% cholesterol is plotted and compared to binding to membranes containing 1 mol% GD1a and 10 mol% cholesterol.



Supplementary Figure 6: Chemical structures of Cholesterol (A) and Cholestenone (B). As noted by the arrows, the only difference between the two structures is the presence of a hydroxyl group versus a ketone.



Supplementary Figure 7: Fluorescence Recovery After Photobleaching (FRAP) of supported lipid bilayers with varying mol % cholesterol. (A) Relative fluorescence recovery after 20-second bleaching of Oregon Green-DHPE in supported bilayers of identical composition (1 mol % GD1a, 0.5 mol % OG-DHPE, 20 mol % DOPE, 0-20 mol % cholesterol and remaining mol % POPC) to those used for influenza binding experiments. (B) Diffusion coefficients for OG-DHPE calculated by fitting fluorescence recovery curves. Fluorescence recovery timescales and thus diffusion coefficients of OG-DHPE in the bilayer were not statistically different for bilayers containing 0, 10, and 20 mol % cholesterol.

References

1. P. M. Kasson, D. L. Ensign and V. S. Pande, *J Am Chem Soc*, 2009, **131**, 1338-1340.
2. T. A. Wassenaar, H. I. Ingolfsson, R. A. Bockmann, D. P. Tieleman and S. J. Marrink, *J Chem Theory Comput*, 2015, **11**, 2144-2155.